Hindawi
Advances in Civil Engineering
Volume 2022, Article ID 7722668, 16 pages
https://doi.org/10.1155/2022/7722668

Research Article

Flexural Behavior of Lattice Girder Slabs with Different Connections: Experimental Study

Yanchun Yun,[1,2] Jiafei Jiang,[3] and Peng Chen[1,2]

[1]*Shanghai Zibao Residential Industry Company Limited, Shanghai 201107, China*
[2]*Baoye Group Company Limited, Shaoxing 312030, China*
[3]*Department of Disaster Mitigation for Structures, Tongji University, Shanghai 200092, China*

Correspondence should be addressed to Jiafei Jiang; jfjiang@tongji.edu.cn

Received 5 May 2022; Revised 30 November 2022; Accepted 5 December 2022; Published 27 December 2022

Academic Editor: Payam Shafigh

Lattice girder slab (LGS) is a precast composite slab that serves as an alternative to conventional concrete-in-place (CIP) slabs. The load-bearing capacity of joints for the LGSs is essential for large-span slabs with precast constructions, while limited connections could achieve both free-of-formwork construction and higher flexural bearing capacity. In order to enhance the flexural behavior of LGSs with free-of-formwork joints, the straight bar lapping connection away from the midspan, loop connection, and straight bar lapping connection within keyway for midspan joints were proposed in this study. Seven full-scale one-way LGSs with different transverse connections were tested under the four-point bending tests to investigate the joint behavior. The overall response and failure mode were observed during the test. The load versus midspan deflection, deflected shape, and characteristic load capacity were analyzed and discussed. The study showed that all the slabs' deformability could reach as high as l/50 without load reduction. The LGS with the straight bar lapping connection in the midspan had the lowest flexural capacity (70% of the capacity for LGS without joints), while the flexural resistance of the slabs with other connections could be increased by 21.4% to 44.6% compared to LGSs with the traditional straight bar lapping connection in the midspan. The LGSs with the connections having keyways had the most significant improvement and could achieve high flexural capacity and 110% of deformability of the LGS without joints. The findings could enrich the connection types for LGSs for construction convenience and mechanical efficiency and further provide reference for the design of the two-way LGSs.

1. Introduction

Precast concrete (PC) structures are advanced structural systems that save construction time, formwork cost reduction, labor work, and energy. Globally, the PC structure is becoming a prevailing structure, and its construction is an important part of green and sustainable development. Regarding the structural system, the PC structures can be classified into precast frame system [1], precast shear wall system [2], and precast frame-shear wall system [3]. The precast slabs are the essential moment-bearing structural components that are primarily subjected to static gravity loads, no matter in which structural system. Nowadays, there are various precast slabs, such as the hollow-core floor, composite slab, solid prestressed composite slab, and so on. Lattice girder slab (LGS) is one of the most commonly used composite slabs (Figure 1). In the LGS system, the precast reinforced plank is temporarily propped in situ and serves as the permanent formwork for the final casting on the top. The usual thickness of precast plank is about 50~65 mm. The bottom floor reinforcement was placed in the precast plank, where the well-spaced 3D lattice girder trusses protrude. The truss element can ensure the stiffness of the precast plank during transportation and hoisting and the capacity of the precast plank during in situ casting. It can also enhance the interface between the precast plank and the CIP concrete topping. The precast reinforced plank can have the benefits of free-fromwork on-site and the lightweight for delivery, hoisting, and installation. Moreover, it can also make it convenient to insert mechanical and electrical components

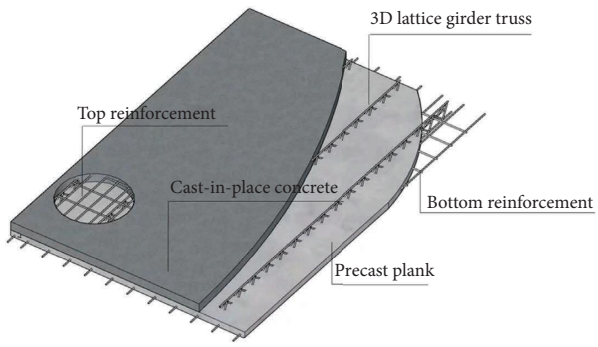

Figure 1: Lattice girder slab.

together with the top layer of reinforcement before casting the top layer.

Usually, the maximum dimension of precast slabs is restricted by the deflection limit of the precast plank and the transportation capacity. Hence, it needs connections to complete the slab system in the structure with pieces of precast planks. Especially for two-way slabs, the connection bearing capacity is essential as the joints are inevitable in one direction of the two-way slab. Eurocode 2 does not speculate on connection details but emphasizes that the joint bending resistance is based on the capacity of the crossbar across the joint and the available lever arm between the crossbar and the concrete compression zone at the top of the cross section [4]. Connections in LGS are specified in the German and Chinese codes. DIN1045 [5] suggested the straight bar lapping connection with two closely attached precast planks for the two-way slab (Figure 2(a)). The truss-type reinforcement is evenly distributed within the lapping zone of standard splice length plus 100 mm. As the crossbar is right upon the surface of the precast planks, the joint bending resistance is reduced with the reduction of effective height. Hence, such a connection is not recommended for the transverse joint in the one-way slab in the Chinese code (GB/T 51231-2016) [6]. In the Chinese code, it is suggested that the CIP concrete strip connection with the lapping system of two longitudinal bars protruding from the precast planks for the joint needs bending resistance (Figure 2(b)). However, the CIP concrete strip connection construction needs additional formwork on site. Therefore, the development of advanced free-of-formwork joints capable of load-bearing is essential for improving the construction efficiency of the precast slab system.

In the existing studies, the flexural performance of LGS was a major concern and has been investigated from the perspective of the performance in the construction stage and the ultimate stage. During the construction stage, the stressing in the precast plank is complex as it experiences three different loading stages: (a) propped before pouring concrete topping, (b) propped while pouring concrete topping until the concrete reaches the required strength, and (c) non-propped after the concrete topping hardens [7]. To better understand the composite behavior during construction, Newell et al. monitored the early-stage performance of two-way LGS in a five-story building [8, 9]. The connections with closely attached precast planks (Figure 2(a)) were adopted in the LGS system. The one-yearreal-time monitoring detected the concrete strain profile before, during, and after pouring the structural concrete topping and demonstrated that the two-way LGS system with the connections could exhibit elastically without cracking at the stage of construction as expected.

The majority of studies focused on flexural performance at the ultimate stage. Since the flexural resistance for two-way action in labs under the plastic hinge line mechanism can be derived from the corresponding one-way flexural behavior of the slab, most parametric studies on the jointed LGSs were conducted on the one-way flexural behavior. Lundgren evaluated the flexural performance in the full-scale LGSs [10]. The author adopted the connections illustrated in Figure 2(a) but without truss elements within the lapping zone in the midspan. The corresponding failure mode was the rupture of reinforcement with a single flexural crack, since the slabs had low reinforcement (0.15%). From the experimental and numerical analysis results, it can be found that the joint without reinforcement would raise the risk of premature brittle failures, as was obtained in similar tests by Tim Gudmand-Høyer [11]. The author also concluded that the joint with the connection in Figure 2(a) is sensitive to flexural cracking and causes brittle failure. Kim and Shim [12] investigated the flexural behavior of half-precast slabs (longitudinal reinforcement ratio between 0.4%~0.67%) for bridges with the loop connection in the midspan and demonstrated that the loop connection was an effective connection for the slab with two closely attached precast planks. The cracking load, flexural capacity, and deflection could be comparable to the slab without joints. Chen et al. [13] investigated the bearing performance of lap-splice connections with additional crossed bent-up rebars (as suggested in Lundgren [10]) in the LGSs (longitudinal reinforcement ratio between 0.61%~1.45%). Their finding was that the bent-up rebar could enhance the interface and anchorage effectiveness of the lap-splice rebar. Hence, the joint could well transfer the force as the monolithic joint. The above-reviewed research focused on the bridge slabs having a thickness of over 200 mm, and the corresponding CIP layer was much thicker than that in the LGSs for buildings. Among the studies on the LGSs with thin thickness, Liu et al. [14] adopted the connection detailing as in Figure 2(a) in the LGSs for building structures. They experimentally investigated the effect of slab thickness, truss element spacing within the lapping zone, and lap length of crossbar on the flexural behavior of one-way LGSs where the connections were in the middle. The test results presented that the truss element within the lapping zone could improve the interface bond and avoid significant detachment as concluded in Stehle et al. [15]. However, the variation of truss element spacing, slab thickness, or lap length of crossbar had a limited effect on load capacity enhancement compared to the LGS without joints. The highest load capacity was 18% lower than the load of the control specimen. Further improvement still needs more reinforcement which may complicate the on-site construction. Ding et al. [16] improved the CIP concrete strip connection in Figure 2(b)

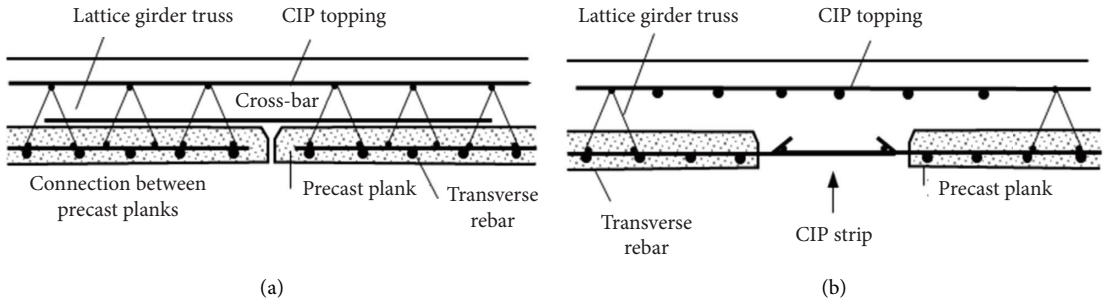

Figure 2: Two types of connections for LGS. (a) Closely attached precast planks [5]. (b) CIP concrete strip [6].

with the bent-up bar to decrease the CIP strip width from 300 mm to 60 mm. The bearing capacity of the jointed slab was close to that of the monolithic slab. However, the formwork below the joint was still needed. According to the existing studies on the flexural behavior of jointed one-way LGSs, the load-bearing connection without formwork still needs improvement.

Moreover, several researchers studied the flexural behavior of two-way LGSs with joints. Zajac et al. [17] compared the flexural behavior of four different two-waysemi-precast concrete slabs under short-term and long-term loading schemes. The common feature was the lack of joint reinforcement. The test observation showed that the LGS without joint reinforcement significantly affected the cracking morphology and the maximum deflections under the long-term loading conditions. The typical defection shape for slabs of the longitudinal joints without reinforcement resulted in a different load distribution factor compared with the in situ slabs [18]. Furthermore, other researchers made efforts to find a way to achieve monolithic equivalence for jointed slabs. Zhang et al. [19] conducted a bending test on a full-scaletwo-way LGS (5 m × 5 m) under a uniformly distributed load. The connection regulated in the DIN1045 code [5] (Figure 2(a)) was designed in the middle joint in one direction. The test results showed that the cracking pattern in the LGS was close to that in the monolithic slab, and the numerical study showed that the crossbar across the joint had a slight effect on increasing the stiffness of the slabs. Chen and Shen [20] introduced the lattice girder truss and the crossbar across the joint to further improve the flexural rigidity and capacity of two-way LGSs, while the performance was not comparable to the CIP slabs in the study. Moreover, other load-bearing connection types have been investigated in other slab systems. Irawan et al. [21] investigated the two-wayhalf-precast slab with two joints in one direction to decrease the bearing demand of connection. Each joint used the triangular rigid connection where a groove with triangular section was formed after assembling precast planks, and bent-up rebar was used as the crossbar. Such a connection has been demonstrated to be equivalent to the monolithic joint in [22]. Irawan et al. concluded that the jointed slab could reach a similar strength as the monolithic slab but had smaller deformability. All in all, there was limited study considering the connection type effect on the flexural behavior of two-way LGSs.

Among the existing studies, it is demonstrated that the improved connection types for LGSs were rather limited. The most efficient way is adding truss elements or using bent-up bars within the lapping zone to avoid interface detachment, while the enhancement is rather limited as the sectional bending capacity of the joint has not been increased. The jointed LGSs cannot be compatible with the monolithic slab or LGS without joints at the ultimate stage, and hence the span of jointed LGS will be limited. In this study, the effect of the number of low-capacity joints (straight bar lapping connection) on the flexural behavior of LGSs was investigated. Additionally, two additional load-bearing connection types (loop connection and straight bar lapping connection within the keyway) were proposed for the LGS. Accordingly, seven full-scaleone-way LGSs were designed to be tested under the static four-point bending test. Two of them were the control specimens, and the remaining five specimens were designed to consider the two factors mentioned above and divided into two groups. The overall response and failure mode were observed during the test. Afterward, the load versus midspan deflection, deflected shape, and characteristic load capacity were analyzed and discussed. The results can help enrich the connection types for LGSs for construction convenience and mechanical efficiency and provide reference for the design of two-way slabs.

2. Specimens and Test

2.1. Specimens. Seven one-way LGSs with identical dimensions were designed based on a multi-rise residential reinforced concrete building prototype, which was designed according to the Chinese concrete structure code (GB 50010-2010). The slab length, width, and thickness were 3000 mm, 780 mm, and 140 mm, respectively (Figure 3). The thickness of precast planks was 60 mm. The surface of the reinforced plank was roughened to achieve a strong interface bond between the precast plank and 80 mm concrete topping. The concrete of precast planks and CIP toppings were designed as the same concrete grade (C30) with the same mix. Hence, one group of concrete cubes for obtaining the concrete strength and modulus was prepared after casting CIP topping, with consideration of the load bearing of slab largely related to the compression strength at the compression zone. The average cubic compressive strength and elastic modulus

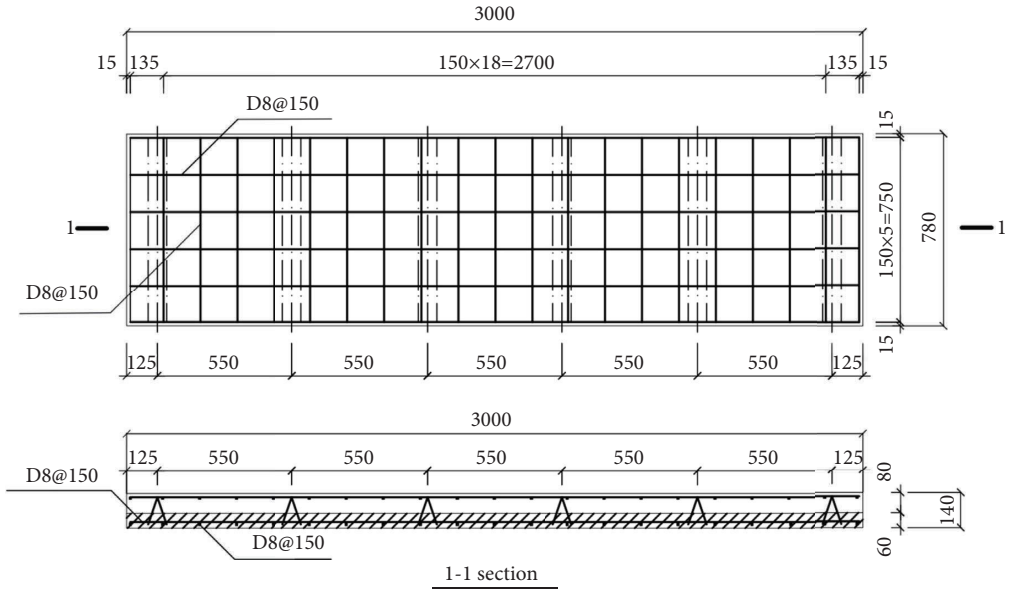

Figure 3: Reinforcement details of LGS01.

were 33 MPa and 32.1 GPa, which were tested during the test. The longitudinal and transverse reinforcement at the precast plank was D8@150 (reinforcement diameter was 8 mm with a spacing of 150 mm). The same reinforcement ratio was adopted in the CIP layer. The reinforcements were HRB400 rebars having yield strength of 454MP, ultimate strength of 612 MPa, and elastic modulus of 206 GPa, obtained by the standard tensile test. It is worth to note that the reinforcement design also meets the requirements of ACI 318 and Eurocode 2.

Seven specimens were divided into three groups. The first group was the control group, including LGS01 and LGS02. LGS01 was the LGS without a joint. Its flexural behavior is the reference of LGS with joints. LGS02 was designed as LGS with the CIP strip connection in the middle. The CIP strip connection had a 300 mm width CIP strip and adopted straight bar lapping with the lap length of l_a (Figure 4(a)), which is the typical monolithic joint with load-bearing capacity for the LGS as regulated in the Chinese code (GB/T512321-2016) [3]. It is the most commonly used joint detailing in engineering practice in China, and its behavior is the direct reference for the LGS with other types of connections. Except for two control specimens, the remaining two groups were the LGSs with connections of closely attached precast planks. They were divided into two groups. In Group A, LGSA1 and LGSA2 used the straight bar lapping connections with the lap length of $1.4l_a$ (Figures 4(b) and 4(c)). Their difference was the location of joints. LGSA1 had the joint in the midspan, similar to the configuration in the existing studies, while LGSA2 had two joints, each at one-third of the slab length and away from the loading point. Group B includes LGSB1, LGSB2, and LGSB3. All of them had the midspan joints but had different connection detailing. LGSB1 had a rectangular loop connection (Figure 4(d)). This connection has been successfully used in the precast concrete shear walls as the vertical connection. The lap length could be reduced to 200 mm, 70% of l_a, which complied with the relevant codes for loop connections [4, 5, 23, 24]. The bent-up legs in the loop could enhance the monolithic behavior of the composite slab by providing shear resistance between the precast and CIP plank interface as the lattice girder trusses. Therefore, the number of truss elements within the joint is reduced by half, resolving the clashing rebar issue. For LGSB2 and LGSB3, the connections were improved by introducing keyways evenly spaced within the lapping zones of each precast plank (Figures 4(e) and 4(f)). Each keyway was 30 mm in depth, 80 mm in width, and 400 mm in length on one side of the precast plank. When two precast planks were assembled in place, two crossbars (D10, its yield strength and ultimate strength were 395 MPa and 614 MPa) were placed in the keyway. For the joint detailing in LGSB2 and LGSB3 (concrete cover for crossbar is 30 mm), it results in the increase of level arm of the crossbar in the keyway which will increase the bending capacity of the joints. In this study, the number of keyways on each precast plank was considered the test variable, that is, two keyways for LGSB2 and three for LGSB3 on one precast plank, respectively. Theoretically, when the keyways are right above the longitudinal reinforcements in the precast plank, all of the level arms of crossbars will increase. However, it will cause the edge of the precast plank to be damaged during transportation and construction. Therefore, the limited number of keyways on each precast plank was considered in the study. It is to be noted that the reinforcement ratio of LGSB2 is the same as that in the control group. The ratio of LGSB3 is higher but with the same ratio in one keyway as that in LGSB2. Detailed information of all the specimens is listed in Table 1.

2.2. Test Program and Measurement. The flexural behavior was tested by the four-point bending test method. The slab was simply supported with a span of 2750 mm. Moreover, the length of the pure bending zone was 1000 mm (Figure 5(a)). The test was first controlled by the load with the constant increment of 2 kN before cracking. Afterward,

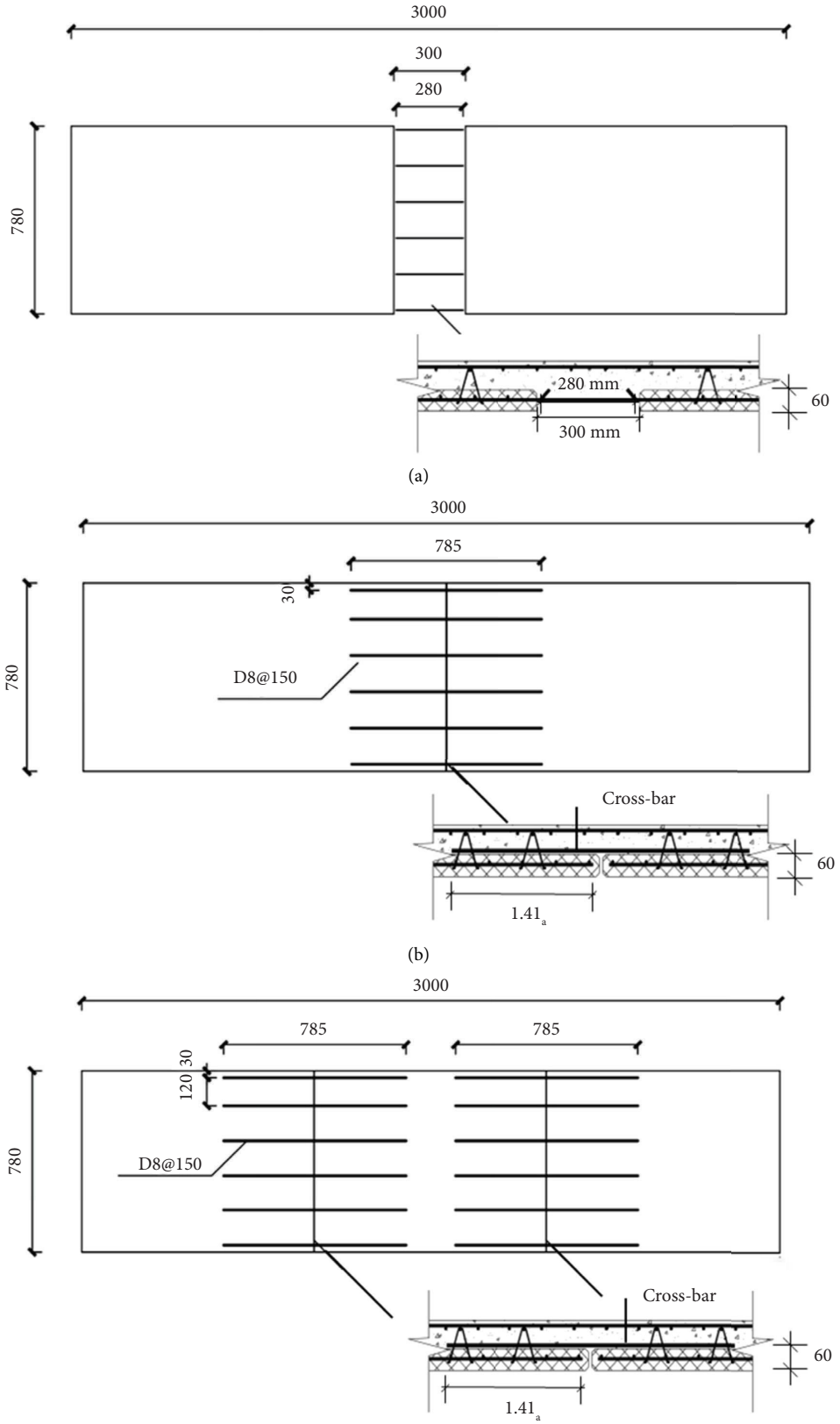

Figure 4: Continued.

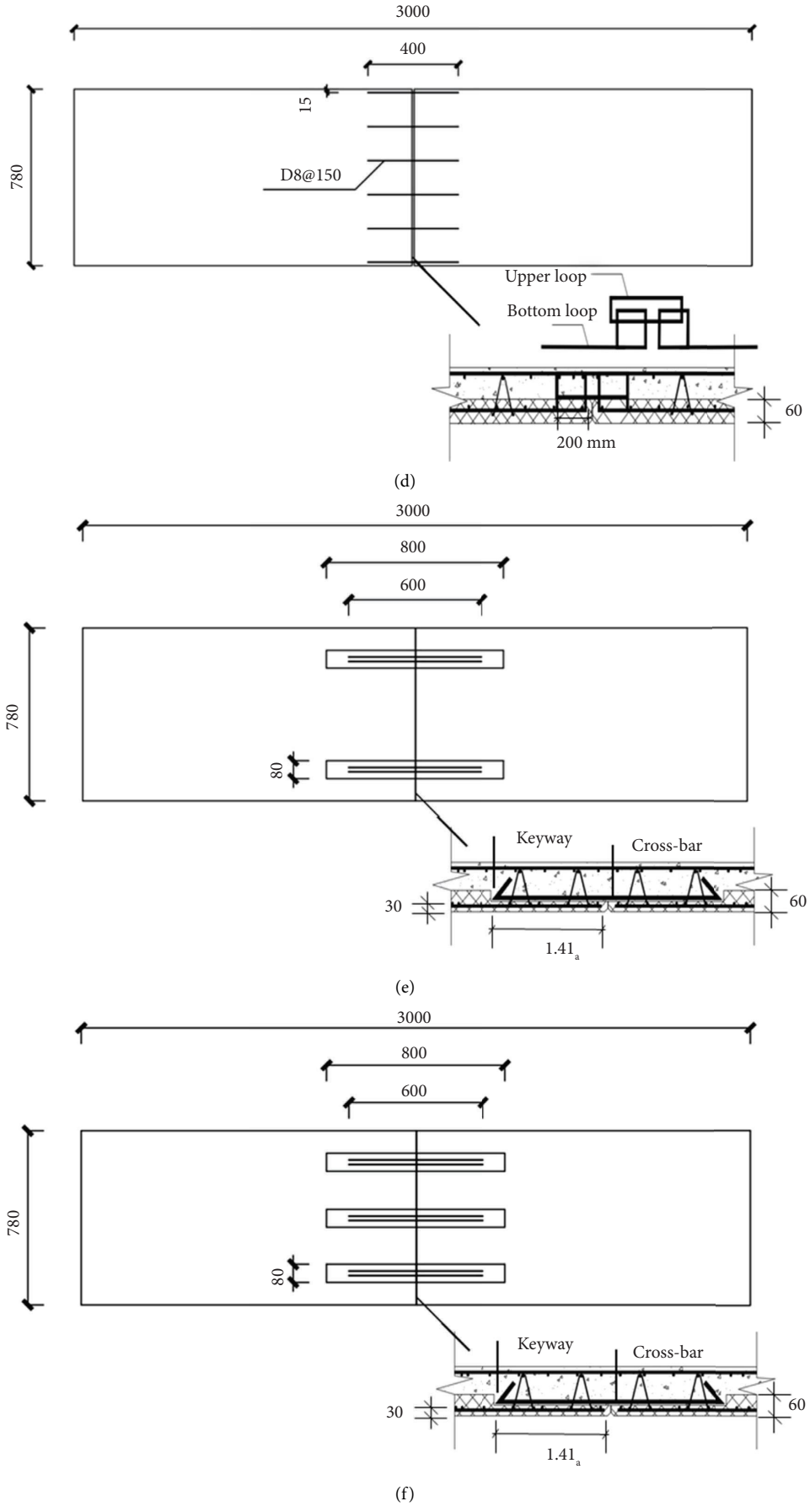

Figure 4: Different connection configurations in specimens. (a) LGS02. (b) LGSA1. (c) LGSA2. (d) LGSB1. (e) LGSB2. (f) LGSB3.

Table 1: Details of specimens.

Group	Specimen ID	Type of precast plank joint	Type of connection	Location of connection	Lapping reinforcement	Lap length/mm
Control group	LGS01	Nil	Nil	Nil	Nil	Nil
	LGS02	CIP strip	Straight bar lapping connection	Midspan	D8@150	280
A (joint location)	LGSA1	Closely attached	Straight bar lapping connection	Midspan	D8@150	392
	LGSA2		Straight bar lapping connection	One-third of slab length	D8@150	
B (connection detailing)	LGSB1	Closely attached	Rectangular loop connection	Midspan	D8@150	200
	LGSB2	Closely attached with two keyways	Straight bar lapping connection	Midspan	2D10 at each keyway	392
	LGSB3	Closely attached with three keyways	Straight bar lapping connection	Midspan		

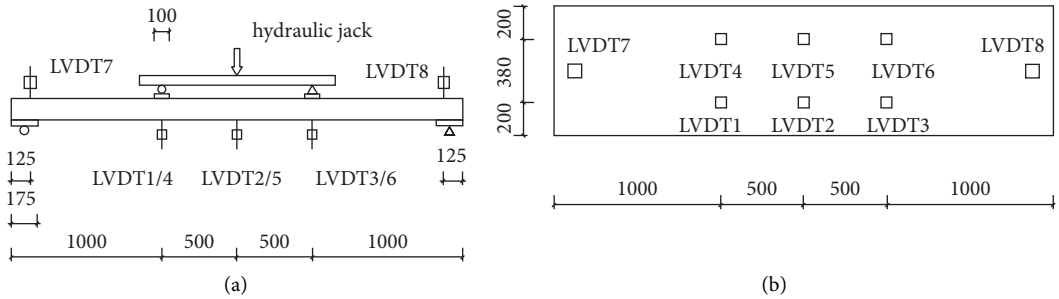

Figure 5: Test setup and instrument. (a) Setup. (b) LVDT layout.

the load increment per step increased to 4 kN (each step interval was 10~15 min varying due to cracking observation). The test scheme follows the sequence as regulated in the Chinese standard for test method of concrete structures (GB 50152-2012). The load rate was 0.3 kN/min. The test program was changed to displace control (0.6 mm/min) when the displacement began to have a fast increment during the load increment. The test would be terminated when the load decreased to 20% of peak load at least.

Eight linear variable differential transducers (LVDTs) were attached to the slab, as illustrated in Figure 5(b). Three pairs of LVDTs detected the deflection at two loading points and the midspan. Another two LVDTs monitored the deformation at the supports to calculate the deflection within the span relative to the end. The load and deflections were recorded by the data log during the test synchronously. Meanwhile, the cracking development was observed with the assistance of the crack monitor to measure the crack width.

3. Test Results and Discussion

3.1. Overall Response. All of the specimens had the flexural failure mode. The significant difference was cracking development which was elaborated as follows.

3.1.1. Control Group. Initially, the deflection of the slab, LGS01, slightly increases with the load. The flexural cracks in the midspan were observed when the load increased to 12.3 kN. No detachment was displayed in the precast plank and CIP topping interface. The flexural cracks developed upwards and crossed the interface with the load increase. More new cracks were generated and evenly distributed in the bending moment zone. After the load increased to 20.1 kN, the load control was switched into displacement control. No new flexural crack could be observed. The existing cracks extended upwards, and the crack width increased with the load. The observed maximum crack width was 1.2 mm in the precast plank. The test was terminated when the load began to decrease at the displacement of 53.5 mm. The final crack pattern is illustrated in Figure 6(a).

The slab, LGS02, had a similar failure process as LGS01, except for cracking development. No crack was observed within the 300 mm CIP strip. The initial crack was generated beside the CIP strip in the precast plank section, which further trigged the horizontal interface cracks. Afterward, more flexural cracks developed, similar to those in the LGS01 but away from the middle. Figure 6(b) illustrates the crack pattern of LGS02. The maximum crack width was 1 mm. The load began to decrease when the midspan deflection reached 53.5 mm. At last, the test was terminated when the midspan deflection was 54.5 mm.

3.1.2. Group A

(1) LGSA1. The initial flexural crack was generated in the midspan of the CIP topping and above the gap between two precast planks when the load increased to 7.8 kN. The

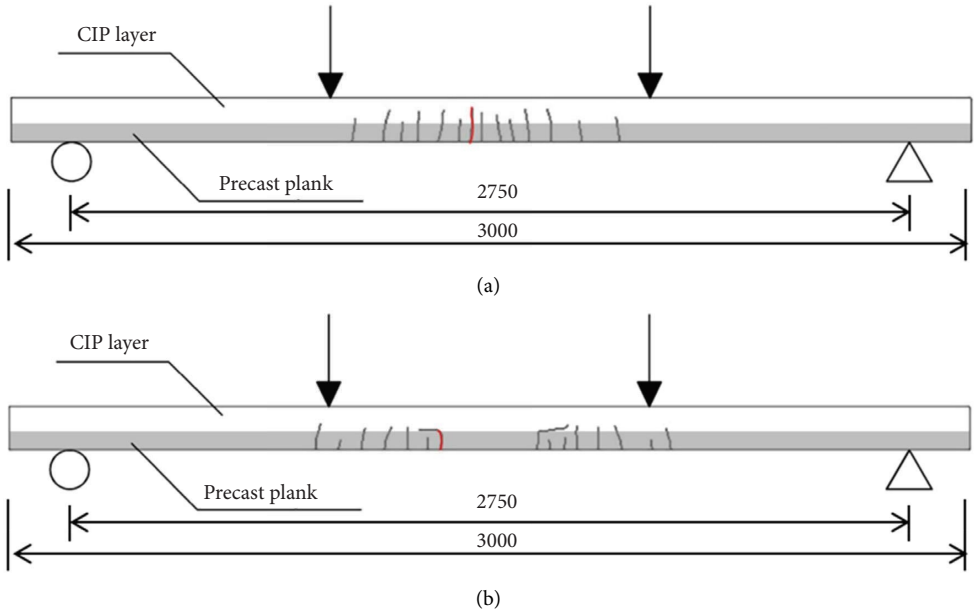

Figure 6: Crack patterns for specimens in the control group. (a) LGS01. (b) LGS02.

cracking load was smaller than LGS01 and LGS02 due to the reduced effective cross section in the middle. At the load of around 12 kN, cracking occurred in the interface starting from the midspan. Afterward, an additional flexural crack was generated around the location of the lattice girder with the extension of the interface crack. Meanwhile, a new flexural crack was also observed in the precast plank (Figure 7(a)). With the load increasing, more cracks were generated in the precast planks out of the lapping zone and with a uniform crack spacing, which was much larger than that in LGS01 and LGS02. Meanwhile, three more flexural cracks with smaller spacing were generated in the CIP topping in the midspan where the interface bond deteriorated. The deflection developed faster when the load increased to 22 kN when the load program was changed to displacement control. The interface opening at the midspan increased with the extension of the interface crack during the load (Figure 7(b)). At this stage, no new crack could be observed. The final crack pattern is illustrated in Figure 7(c). The maximum flexural crack (above the joint) width was 1.6 mm. Finally, the load reached the peak value when the deflection increased to 75.35 mm.

(2) LGSA2. The initial flexural crack was generated in the midspan of the CIP topping at the load around 8 kN; afterward, the interface crack was observed. At the load of 14.1 kN, two additional flexural cracks next to the location of truss girders were developed in the CIP topping of two connections after the extension of interface cracks (Figure 8(a)). Cracking development in the precast plank was observed when the load increased to 20 kN (Figure 8(b)). The load control program was shifted to the displacement control when the load increased to 35 kN. The slab began to have excessive development in deflection and slow increment in load capacity. No new crack was generated, and the crack width increased faster in the connecting region than in the area between two connections. The maximum flexural crack was at CIP layer above one joint. The width observed was 1.2 mm, slightly smaller than that in LGSA1. Finally, the test was stopped when the load began to drop at the deflection of 60.8 mm. The final crack pattern is shown in Figure 8(c).

To sum up, LGSA1 and LGSA2 had a significant difference in the crack pattern compared with the two control specimens. In LGSA1 and LGSA2, the cracks in the CIP toppings within the lapping zones had three flexural cracks associated with interface cracking between two adjacent cracks, and the spacing of adjacent flexural cracks was determined by the location of the truss girder in the lapping zone. Due to smaller cross section stiffness within the lapping zone, the crack spacing was smaller than that out of the lapping zone. The connection moving apart from the midspan alleviated the cracking in the pure bending zone during the loading and reduced the cracking opening of interface crack at the connections. Therefore, the change of connection location resulted in LGS02 having lower curvature in the pure bending zone, the deflected shape of which is demonstrated in Section 3.3.

3.1.3. Group B

(1) LGSB1. At the load of 9.6 kN, the interface crack was observed next to the panel joint. The initial flexural crack was observed in the CIP topping at the midspan when the load increased to 11.3 kN (Figure 9(a)). The development of cracks in the precast planks had not been recorded until the load increased to 16 kN (Figure 9(b)). These cracks extended into the CIP topping, as observed in the other composite slabs. After no new crack was observed, the deflection developed faster, associated with the crack width increase. At this stage, the displacement control controlled the test until

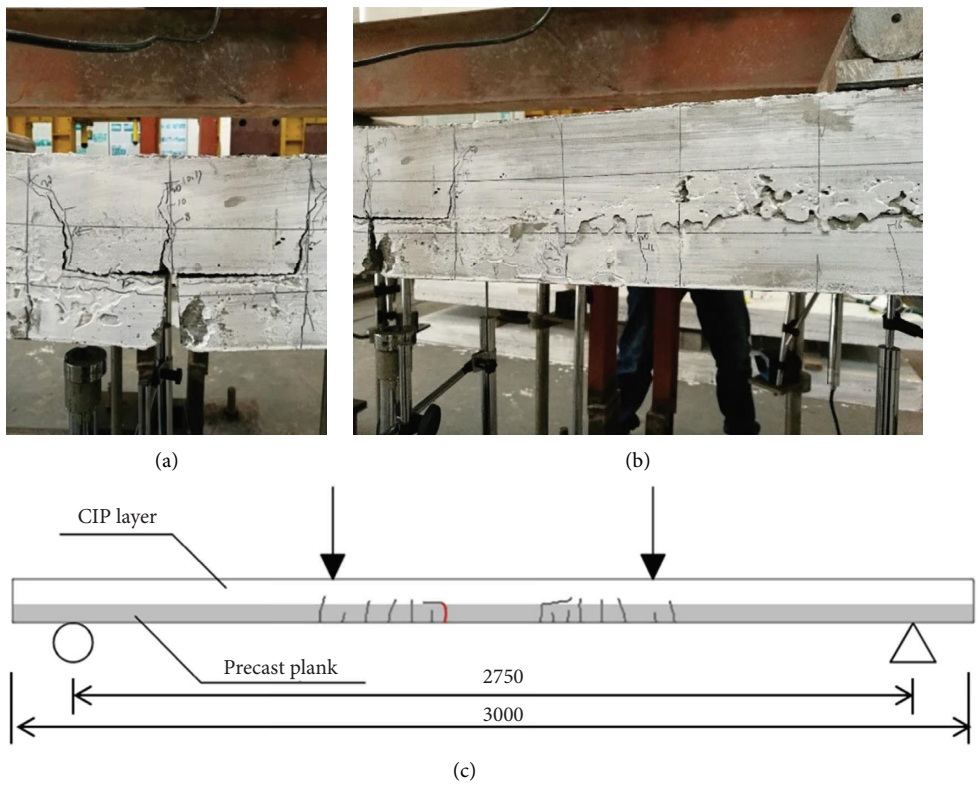

Figure 7: Failure phenomenon of LGSA1. (a) Cracking at midspan. (b) Cracking in the precast plank. (c) Crack pattern.

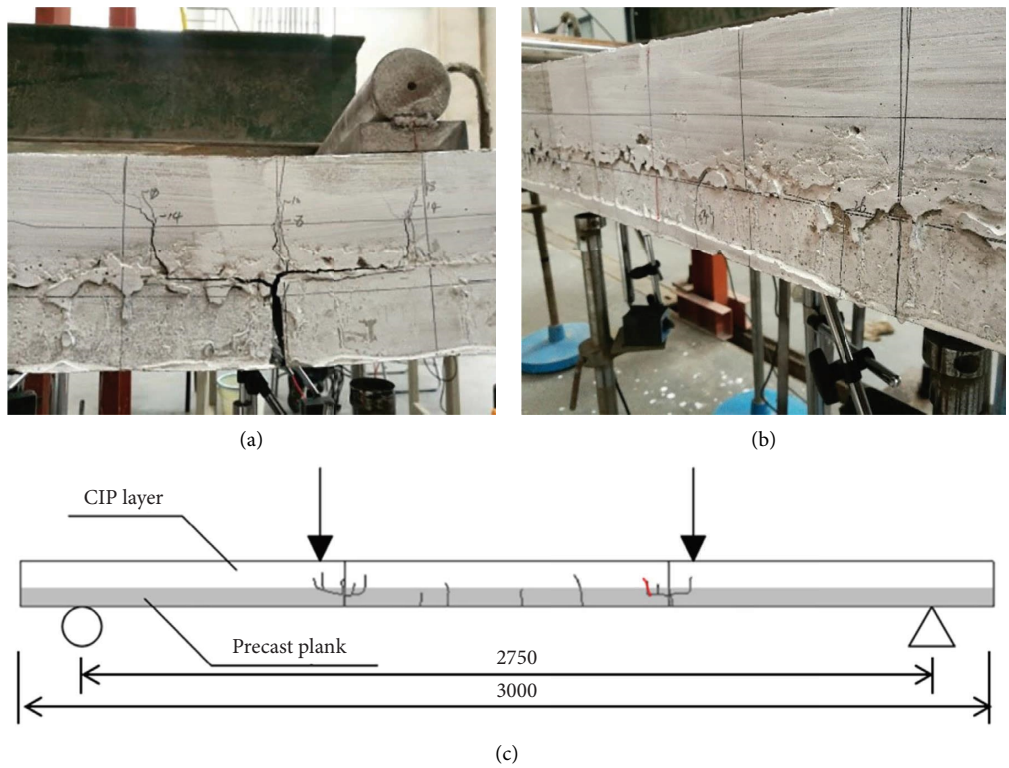

Figure 8: Failure phenomenon of LGSA2. (a) Cracking at one joint. (b) Cracking at midspan. (c) Crack pattern.

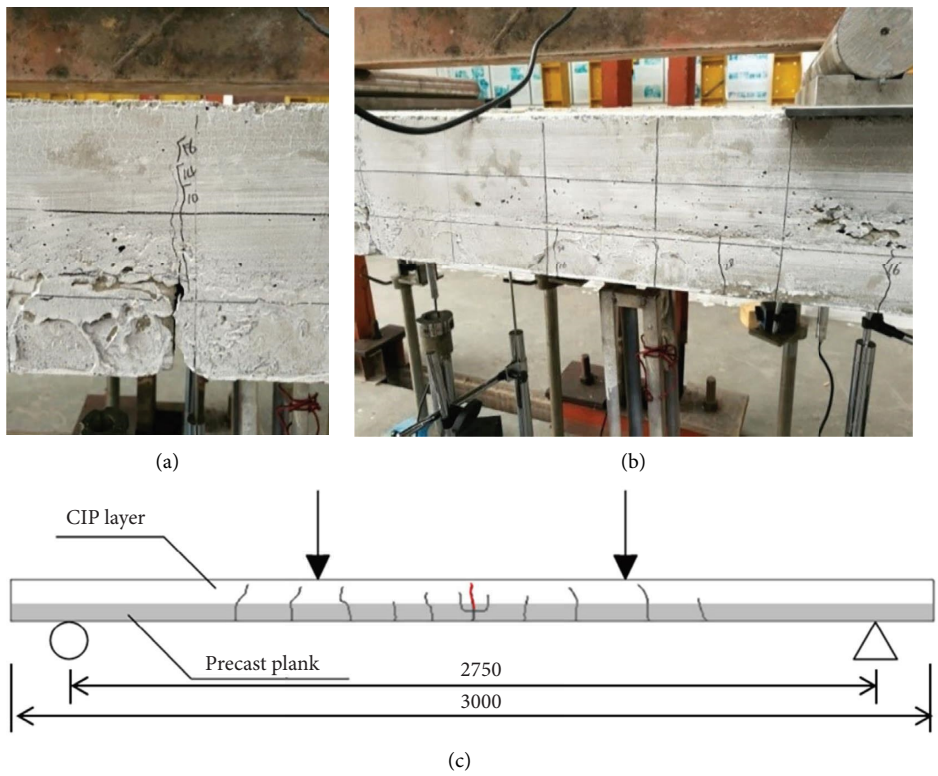

Figure 9: Failure phenomenon of LGSB1. (a) Cracking at midspan. (b) Cracking in the precast plank. (c) Crack pattern.

the load dropped at the deflection of 65.5 mm. The crack pattern is illustrated in Figure 9(c). The critical crack was the flexural crack in the midspan. The maximum crack width was 1.4 mm. Compared with LGSA1, LGSB1 had a similar crack pattern but a relatively shorter length and width of interface crack.

(2) LGSB2. The initial flexural crack was first observed in the CIP topping at the midspan at the load of 7.4 kN. Simultaneously, the interface cracking was also observed (Figure 10(a)). When the load increased to 16 kN, more flexural cracks were generated in the precast plank. Also, these cracks crossed the interface and developed in the CIP topping when the load increased to 20 kN. Meanwhile, a few cracks were generated within the shear span. After the load reached 26 kN, no new crack was observed, and the load mode was changed to displacement control mode. Meanwhile, a significant extension of flexural crack was observed around the loading points (Figure 10(b)). After the load began to stop at the deflection of 69.1 mm, the final crack pattern was recorded, as shown in Figure 10(c). The maximum flexural crack was located in the midspan. The crack width was around 2 mm.

(3) LGSB3. The specimen had an identical failure process as LGSB2 but had different critical load values corresponding to the specific stage. The initial flexural and interface crack load was around 9.6 kN (Figure 11(a)). The flexural cracks in the precast plank were observed at the load of 18 kN and developed into the CIP topping when the load reached 24 kN (Figure 11(b)). Similar to LGSB2, a few cracks were observed within the shear span. After the load reached 31 kN, the load program was controlled by the constant displacement rate until the failure of the specimen at the deflection of 60.0 mm. The final crack pattern is illustrated in Figure 11(c). The maximum crack was the flexural crack under one loading point. The crack width was around 1.4 mm.

All in all, three different connection detailing measures had not caused a significant difference in the crack patterns. Similar to the specimens in Group A, the "ш" shape crack pattern was observed at the joints. The development length of interface cracking in LGSB1, LGSB2, and LGSB3 was rather smaller than that in LGSA1. Especially, the interface cracking was significantly restrained in LGSB1 due to the relatively significant dowel effect from the rectangular loops. Moreover, there were fewer flexural cracks in the specimens of Group B than LGSA1. The setting of keyways significantly reduced the flexural cracks as its effect enhanced the effective height and stiffness, which also improved the flexural resistance. Therefore, a few shear-flexural cracks were generated in LGSB2 and LGSB3. The number of keyways had no significant effect on the crack pattern but had a significant effect on the load-deflection behavior. A detailed explanation will be presented in the following sections.

3.2. Load versus Midspan Deflection. The flexural behavior of LGSs with different connections was evaluated and compared by the load-deflection curves (Figure 12), where the load referred to the data from the load cell under the hydraulic jack (Figure 5), and the deflection was the midspan deformation corrected by deformation at two supports. All

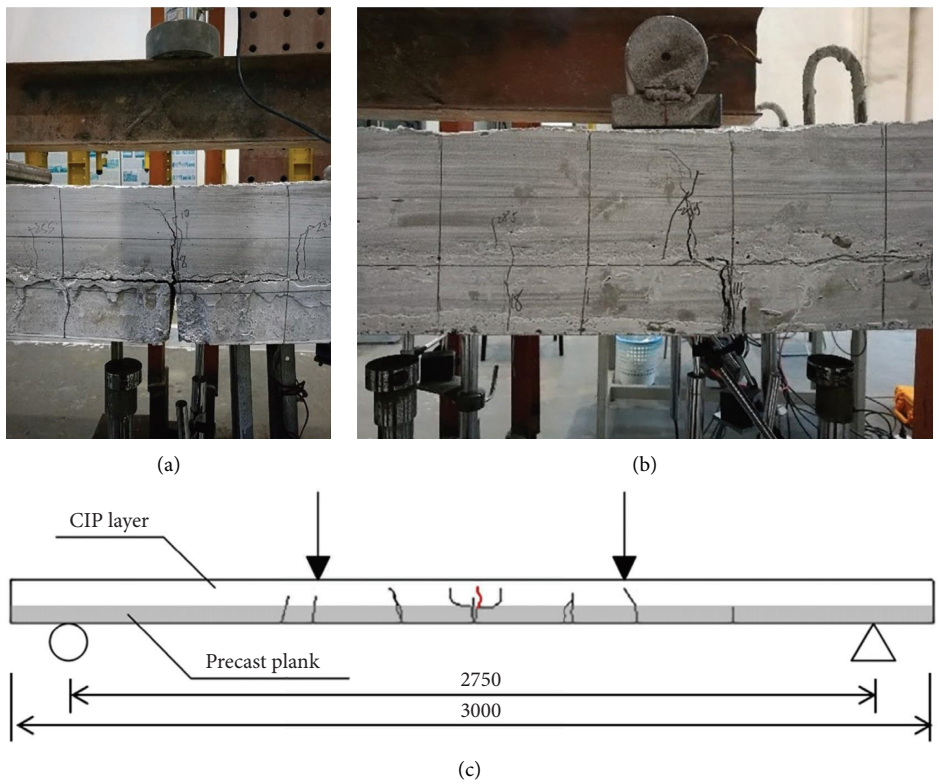

Figure 10: Failure phenomenon of LGSB2. (a) Cracking at midspan. (b) Cracking in the precast plank. (c) Crack pattern.

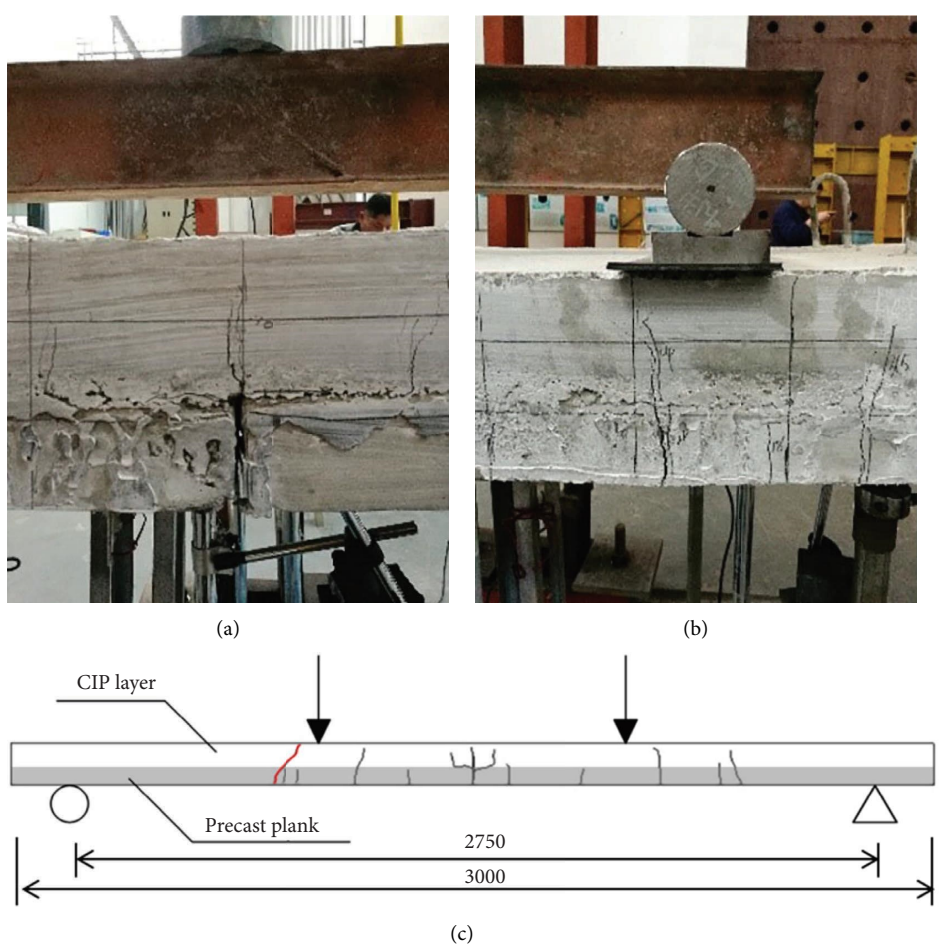

Figure 11: Failure phenomenon of LGSB3. (a) Cracking at midspan. (b) Cracking in the precast plank. (c) Crack pattern.

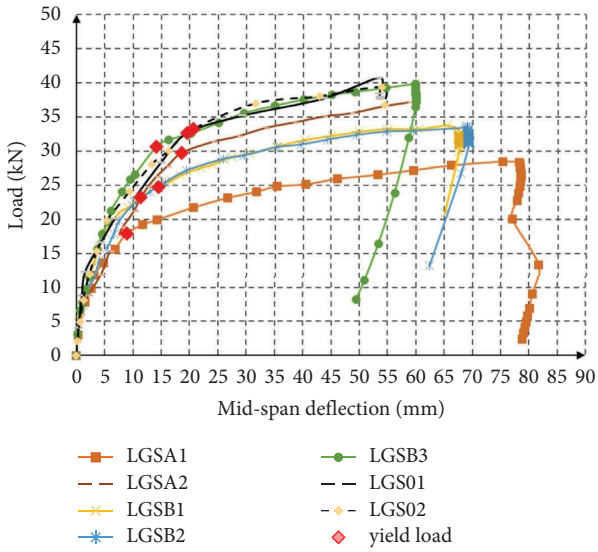

Figure 12: Load-deflection curve.

the curves exhibited three-stage behavior. Initially, the uncracked slab had the linear load versus deflection relationship, determining the initial stiffness. From the figures, it could be found that different connection configurations had a minor effect on the initial stiffness. After it cracked, the slope of the load-deflection curve began to reduce. This stage stopped at the yield point, determined by the graphical method (see Section 3.4). After that point, the curve development stepped into the third stage when it had excessive deflection and minor load increment.

Two control specimens had identical load-deflection curves. Therefore, the CIP strip (LGS02) connection enabled the slab to work as the monolithic LGS. Among the LGSs (Groups A and B) with the connections of closely attached planks, LGSA1 had the lowest flexural stiffness and capacity The reduction of cross section height in the midspan caused the sectional flexural stiffness to be reduced by 81.3% (cross section height reduced from 140 mm to 80 mm), which further induced the excessive curvature increment in the joint and detachment along the interface initiated from the gap (Figure 13). Such a phenomenon has also been observed in other references [7, 16, 20]. The interface detachment would reduce the bond transfer length and limit the stressing in the crossbar. Comparatively, LGSA2 had a smaller deflection and sectional curvature in the joint. It reduced the interface normal stress and detachment length as shown in Figure 8(a). The ultimate stress in the crossbar could be less restricted by the interface detachment, which increased the ultimate flexural capacity compared to LGSA1. However, the capacity of LGSA2 was still less than the monolithic slab as the effective height of the joint section was smaller.

The load-deflection performance of the LGSs in Group B was much better than that of LGSA1. For LGSB1, the detailing of the rectangular loops improved the interface resistance through the dowel effect, which further restrained the interface cracking and alleviated the deterioration of load

Figure 13: Interface detachment and stress in crossbar [25].

transfer in the lapping system. Hence, the connection's flexural capacity could be improved compared to LGSA1. In comparison, the detailing in LGSB2 was designed to increase the effective cross section height at the joint with the keyway and increase the load capacity. The results showed that two types of connections could make the LGSs have close load-deflection curves and similar enhancement effects. However, the improvement was not as much as that in LGSA2. The load capacity was still lower than that of control specimens. Furthermore, the design of LGSB3 considered the effect of increasing cross section area in the transverse direction with the increase of keyways. The comparison between LGSB2 and LGSB3 showed that increasing keyways which resulted in the increase of reinforcement ratio could significantly enhance flexural performance. The load-deflection curve of LGSB3 could be comparable to that of LGS01 and LGS02. Moreover, the enhancement could also be attributed to the increment of the reinforcement ratio from 2.8% to 5.7%. The increment was to ensure the same detailing in each keyway between LGSB2 and LGSB3.

3.3. Deflected Shape of the Slabs. Based on a group of LVDTs installed at different positions (Figure 5), the deflected shape of the slabs could be drawn at a specific load step, as shown in Figure 14. Herein, two load stages were selected for comparison, the yield load and the peak load stage. The former was regarded as the ending of the elastic stage, where no significant non-linear deformation occurred. The determination of the yield point has been elaborated in Section 3.4. The deflection ratio of the average deflection at 1/3 and 2/3-span to the midspan deflection was defined to evaluate the deflected shape difference (Table 2). Accordingly, the closer to 0.63 the ratio is, the more linear the deflection curve between the support and midspan is, demonstrating the midspan section forming a hinge.

At the yield load stage, two control specimens had much larger deflection and higher deflection ratios compared with other specimens. In Group A, LGSA1 had the lowest deflection ratio closer to 0.63. The excessive deformation concentrated in the middle was caused by the flexural stiffness of the joint section which was much smaller than that of the section out of joint, which took effect at the service load stage. When the joint moved to the 1/3-span at each side, the excessive deformation within the joint was significantly alleviated. The deflection of LGSA2 at the joints turned closer to the deflection of LGS01 and LGS02 at the same location. On the contrary, the deflected shape pattern of the specimens in Group B was similar to that of the control specimens. Although the deflection values were smaller than those in LGS01 and LGS02, the deflection ratios were closer to the ratios in the two control

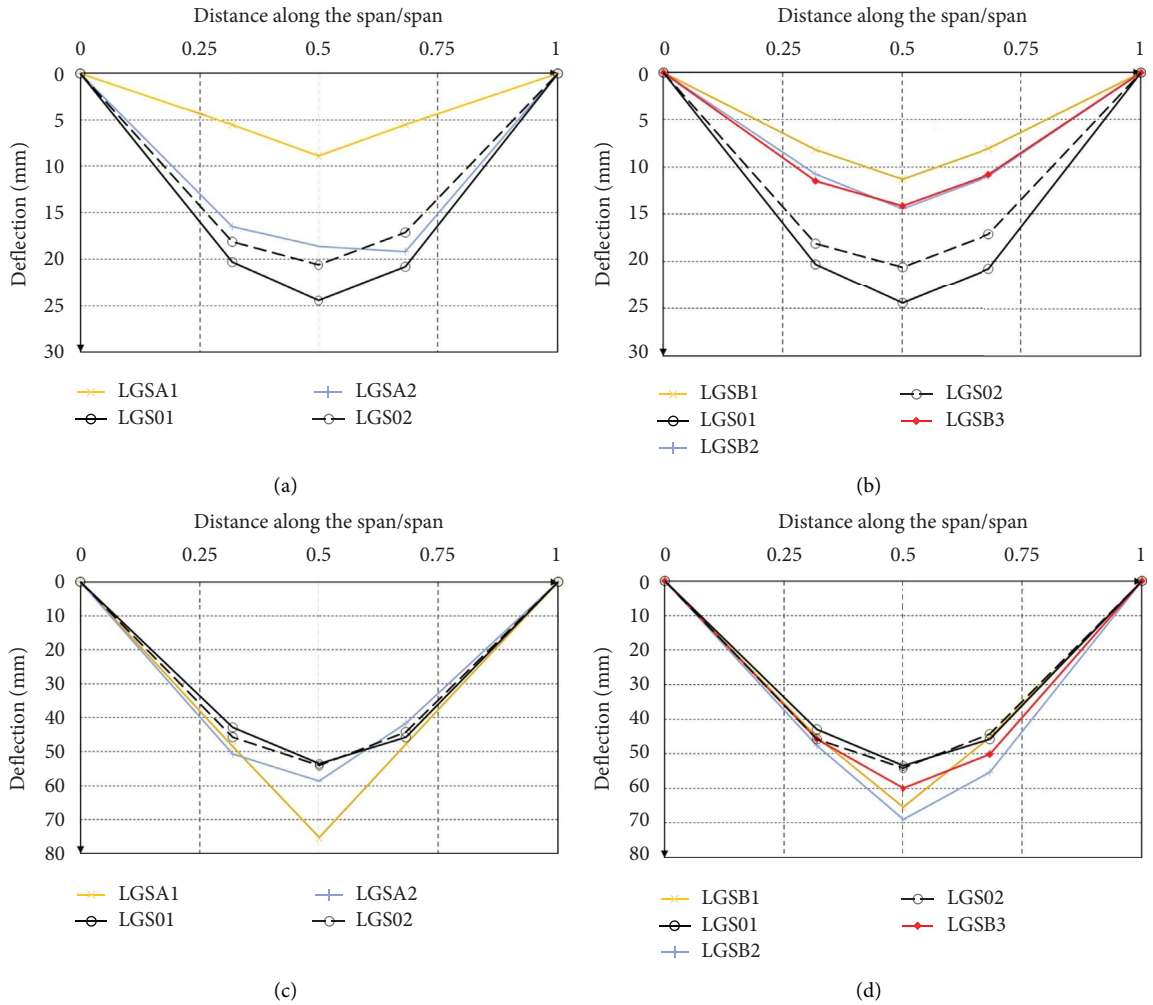

Figure 14: Deflected shape of specimens with comparison of control specimens. (a) Specimens in Group A at yield load. (b) Specimens in Group B at yield load. (c) Specimens in Group A at peak load. (d) Specimens in Group B at peak load.

Table 2: Deflection ratio of specimens.

Spec. ID	LGS01	LGS02	LGSA1	LGSA2	LGSB1	LGSB2	LGSB3
Yield load	0.84	0.85	0.62	0.96	0.76	0.79	0.80
Peak load	0.82	0.83	0.64	0.79	0.68	0.75	0.80

specimens. The deflection ratio of LGSB1, LGSB2, and LGSB3 was 9.5%, 5.9%, and 4.8% lower than the ratio of LGS01, respectively. The connection detailing improvement had enhanced the joint flexural stiffness and alleviated the stiffness difference along the span before the rebar yield.

At the peak load stage, the deflection difference among LGSs in Groups A and B and control groups turned out to be minor compared with the service load stage performance. Two control specimens, LGS01 and LGS02, had identical deflected shapes with the deflection ratios of 0.82 and 0.83, respectively. The ratio had no significant difference for specimens at service load and peak load stage. It further demonstrated that the CIP strip joint between precast planks could enable the jointed LGS to achieve monolithic behavior as the LGS without joints. Regarding the jointed LGS with closely attached planks (LGSA1 and LGSA2), the deflection at the midspan was higher than that of LGS01 and LGS02. LGSA1 had the highest deflection at the midspan and the lowest deflection ratio. The joint location adjustment in LGSA2 could alleviate the excessive deformation in the midspan by setting two joints away from the midspan. Its deflection ratio was improved by 25% and was 3.6% lower than that of LGS01. In Group B, the connection detailing improvement had increased the deflection ratio of LGSB1, LGSB2, and LGSB3 by 7.9%, 19.0%, and 25.4% compared with LGSA1, respectively. The most effective improvement was LGSB3, which had a deflected shape comparable to LGS01 and LGS02. In other words, the effective cross section depth increase was the most efficient way to recover the flexural stiffness comparable to that in the LGS without joints.

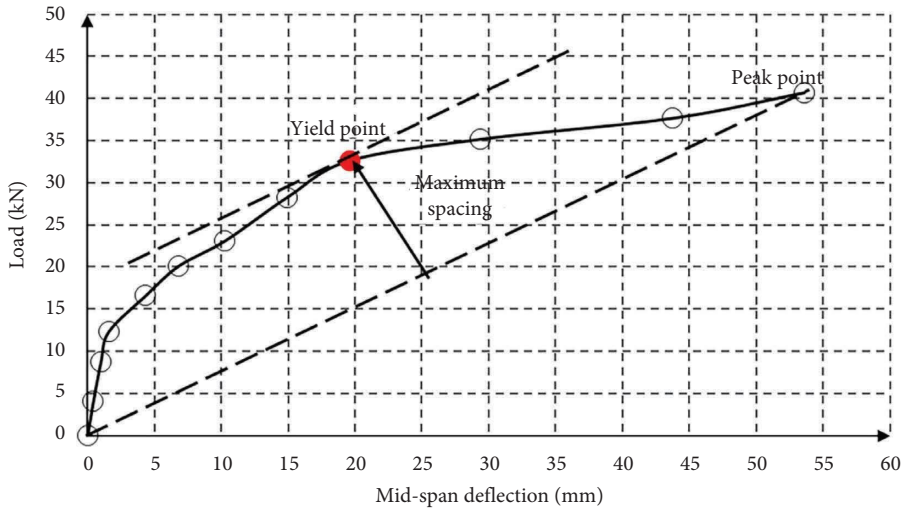

Figure 15: Farthest point method [26].

3.4. Characteristic Load and Corresponding Deflection. As described in Section 3.1, the load-deflection performance could be evaluated by the cracking load, yield load, peak load, and corresponding deflection. In this study, since the rebar strain gauges were out of work during the test, the yield load was determined by the farthest point method proposed by Feng et al. [26] (illustrated in Figure 15). It can be found in Figure 12 that the predicted yield point was also the turning point which was consistent with the feature observed in other studies by the yield strain in the rebar [27–29]. In general, all the characteristic values of the specimens are summarized in Table 3.

3.4.1. Cracking Load. The cracking loads of LGS specimens in Groups A and B were between 8 and 10 kN, 22 to 40% and 37 to 51% lower than those of LGS01 and LGS02, respectively. It can be attributed to the reduction of effective cross section height and the flexural stiffness in the specimens of Groups A and B. LGSB1 and LGSB3 had a slightly higher cracking load (flexural cracking associated with interface cracking) due to the dowel effect of loop reinforcement and higher reinforcement ratio, respectively. In general, the different connection configurations for closely attached planks had a minor effect on the cracking load.

3.4.2. Yield and Peak Strengths. Two controlling specimens had similar yield and peak strength with a 2 to 4% difference. LGSA1 had the lowest yield and peak strength compared with other specimens. The yield and peak values were 45.6% and 32.2% lower than the corresponding average values in the control group. When the connection configuration, the same as in LGSA1, was set at one-third and two-thirds of the span, the yield load and peak load were significantly increased by 65.9% and 36.9%, respectively. Moreover, the difference to that of controlling specimens was reduced to be within 10%. In Group B, LGSB1 and LGSB2 had close yield and peak strength with a difference of 6.5% and 0.9%, respectively. They were around 25% and 17% lower than the average yield and peak strength of LGS01 and LGS02. Compared with the connection type in LGSA1, the rectangular loop connection and keyway configuration enhanced the yield and peak load capacity by over 30% and 20%, respectively. The enhancement of joint bearing in LGSB1 and LGSB2 can be attributed to the loop confinement on concrete and level arm increment in the crossbar. Among all the jointed LGSs, LGSB3 had the best performance. The yield load and peak load were only 7% and 2% lower than the average yield and peak load of slabs in the control group, respectively.

Moreover, the cross section analysis was conducted to compare the flexural capacity values between test and analytical values (Table 3). The strength of the jointed slab is calculated after the determination of the arm level of the crossbar. It can be found that the controlling specimens and LGSB3 could be well predicted. Hence, LGSB3 behaved as a monolithic slab, while the flexural capacities of the other LGSs were underestimated. LGSA2 and LGSB1's prediction differences are much larger than the difference for LGSA1. It can further demonstrate that the measures in LGSA2 and LGSB1 can have a significant effect on alleviating interface detachment between CIP and precast layers. It is because the interface detachment effect has been fully considered in the analytical formulas, that is, the contribution of the precast layer and the reinforcement has not been considered in the flexural resistance. Further studies will be needed to establish the analytical method to adequately consider the interface performance in the jointed LGSs.

3.4.3. Deflection at the Midspan. From Table 3, it can also be found that the connection with higher bearing capacity caused the slab with smaller ductility. In other words, the improvement measures had a more significant enhancement effect on flexural stiffness, especially for the secant stiffness corresponding to the yield point. However, all of the specimens in Groups A and B had ductility ratios larger than 3. Meanwhile, all the specimens in Groups A and B had relatively larger deformability than the control specimens and exceeded the slab deflection limit ($l/50 = 1/50^{*}2750 =$

Table 3: Characteristic properties of LGS specimens.

Specimen ID	Cracking load (kN)	Yield load (kN)	Peak load (kN)	Theoretical load (kN)	Test/ prediction	Δ_y (mm)	Δ_{max} (mm)	Ductility
LGS01	12.3	32.62	40.7	41.1	1.0	19.57	53.5	2.73
LGS02	15.3	33.18	39.3	41.1	1.0	20.59	54.1	2.63
LGSA1	7.8	17.9	28.4	22.4	1.3	8.9	75.4	8.47
LGSA2	8.8	29.7	37.1	24.0	1.5	18.6	60.8	3.27
LGSB1	9.6	23.2	33.7	22.4	1.5	11.3	65.5	5.8
LGSB2	7.4	24.7	33.6	28.9	1.2	14.4	69.1	4.8
LGSB3	9.6	30.6	39.2	42.6	0.9	14.1	60	4.25

55 mm). Therefore, the improvement of connection detailing had no significant adverse effect on the deflection performance.

4. Conclusion

In this study, seven full-scaleone-way lattice girder slabs were designed to investigate the effect of connection position and connection type on the flexural performance of LGSs. The conclusion is summarized as follows:

(1) The position adjustment of joints with the straight bar lapping connections could improve flexural capacity and deflection development. When the joint was set at one-third of the slab length, the capacity could reach 91.1% of LGS01 and LGS without joints and was 30.6% higher than that of LGSA1.

(2) The loop connection could improve the interface shearing resistance through the dowel effect and alleviate the deterioration of load transfer in the lapping system. Consequently, the flexural capacity was improved by 22.5% compared with LGSA1.

(3) The measurement of the keyway could increase the effective height directly and hence the flexural capacity and deformability. The test demonstrated that the three-keyway measurement with a higher reinforcement ratio could ensure that the slab was comparable to the LGS without joints. The flexural capacity was 38% higher than that of LGSA1.

To sum up, both the position of joint and reinforcement detailing improvement could improve the flexural performance of one-way LGSs with closely attached precast planks. The current study qualitatively investigated the flexural behavior of one-way LGSs with different improved connections. Numerical studies will be our further work to optimize the connection design for the LGSs by the parametric study from the finite element model (FEM) with consideration of the non-linearity of concrete and steel and interface behavior between precast plank and CIP topping. The FEM will further investigate the flexural behavior of two-way LGSs with optimized connections.

Data Availability

The data used to support the findings of this study are available from the corresponding author upon request.

Conflicts of Interest

The authors declare that they have no conflicts of interest.

Acknowledgments

The authors gratefully acknowledge the financial support provided by the National Natural Science Foundation of China (grant no. 51978503) and the National Key Research Program of China (Technology Boosting Economy 2020).

References

[1] M. Song, J. He, Y. Liu et al., "Seismic behavior of three-story prestressed fabricated concrete frame under dynamic and low reversed cyclic loading," *Advances in Civil Engineering*, vol. 2018, Article ID 7876908, 10 pages, 2018.

[2] J. Jiang, J. Luo, W. Xue, X. Hu, and D. Qin, "Seismic performance of precast concrete double skin shear walls with different vertical connection types," *Engineering Structures*, vol. 245, Article ID 112911, 2021.

[3] K. Xia, X. Hu, and W. Xue, "Experimental studies on in-plane connections of composite beam-precast concrete shear wall under reversed cyclic loading," *Structures*, vol. 34, pp. 1961–1972, 2021.

[4] C. Européen, *Eurocode 2 EN-1992-1-1: Eurocode 2: Design of Concrete Structures: Part 1-1: General Rules and Rules for Buildings*, London: British Standard Institution, London , UK, 2008.

[5] DIN (Deutsches Institut für Normung), *DIN 1045-1: 2008-08 Concrete, Reinforced and Prestressed concrete Structures –Part 1: Design and Construction*, German Institute for Standardisation, Berlin, Germany, in Germany, 2008.

[6] MOHURD, "Technical standard for assembled buildings with concrete structure," China Architecture & Building Press, Beijing, China, GB/T 51231-2016, 2016.

[7] I. Löfgren, "Lattice Girder Elements in Four point Bending–Pilot experiment," Report No. 01:7, Chalmers University of Technology, Göteborg, Sweden, 2001.

[8] S. Newell, J. Goggins, M. Hajdukiewicz, and D. Holleran, "Behaviour of hybrid concrete lattice girder flat slab system using insitu structural health monitoring," in *Proceedings of the Civil Engineering Research in Ireland (CERI 2016)*, Galway, Ireland, August 2016.

[9] S. Newell and J. Goggins, "Investigation of thermal behaviour of a hybrid precasted concrete floor using embedded sensors," *International Journal of Concrete Structures and Materials*, vol. 12, no. 1, pp. 66–21, 2018.

[10] K. Lundgren, "Lap splice over a grouted joint in a lattice girder system," *Magazine of Concrete Research*, vol. 59, no. 10, pp. 713–727, 2007.
[11] T. Tim Gudmand-Høyer, *Forsøg vedr. Momentkapaciteten af enspeciel samling i bubble deck*Danmarks Tekniske Universitet, Kongens Lyngby, Denmark, 2003.
[12] D. W. Kim and C. S. Shim, "Crack width control on concrete slab using half-depth precast panels with loop joints," *Journal of the Korean Society of Civil Engineers*, vol. 35, no. 1, pp. 19–29, 2015.
[13] Y. Chen, H. R. Shi, C. L. Wang, J. Wu, and Z. Q. Liao, "Flexural mechanism and design method of novel precast concrete slabs with crossed bent-up rebar," *Journal of Building Engineering*, vol. 50, Article ID 104216, 2022.
[14] Y. L. Liu, J. Q. Huang, X. Chong, and X. Ye, "Experimental investigation on flexural performance of semi-precast reinforced concrete one-way slab with joint," *Structural Concrete*, vol. 22, no. 4, pp. 2243–2257, 2021.
[15] J. Stehle, A. Kanellopoulos, and B. L. Karihaloo, "Performance of joints in reinforced concrete slabs for two-way spanning action," *Proceedings of the Institution of Civil Engineers-Structures and Buildings*, vol. 164, no. 3, pp. 197–209, 2011.
[16] K. Ding, C. Dong, Y. Liu, and S. Xia, "Theoretical and experimental study on mechanical behavior of laminated slabs with new type joints," *China Civil Engineering Journal*, vol. 48, no. 10, pp. 64–69, 2015, in Chinese.
[17] J. Zając, Ł Drobiec, R. Jasiński et al., "The behaviour of half-slabs and hollow-core slab in four-edge supported conditions," *Applied Sciences*, vol. 11, no. 21, Article ID 10354, 2021.
[18] J.-Y. Song, E. Kim S, H. Lee, and H. G. Kwak, "Load distribution factors for hollow core slabs with in-situ reinforced concrete joints," *International Journal of Concrete Structures and Materials*, vol. 3, no. 1, pp. 63–69, 2009.
[19] X. Zhang, H. Li, S. Liang, and H. Zhang, "Experimental and numerical study of lattice girder composite slabs with monolithic joint," *Crystals*, vol. 11, no. 2, p. 219, 2021.
[20] C. Dong and X. Shen, "Study on loading mechanism of bi-directional self-supporting concrete composite plates with truss rebar," *Building Structure*, vol. 15, pp. 93–96, 2015, In Chinese.
[21] D. Irawan, D. Iranata, and P. Suprobo, "Experimental study of two way half slab precast using triangular rigid connection of precast concrete component," *International Journal of Applied Engineering Research*, vol. 12, no. 5, pp. 744–754, 2017.
[22] S. Wijanto and T. Takim, "State of the Art: Research and Application of Precast/Prestressed concrete Systems in Indonesia," in *Proceedings of the 14th World Conference on Earthquake Engineering*, Beijing, China, October 2008.
[23] American Concrete Institute, "Building code requirements for structural concrete and commentary," *ACI Committee*, Vol. 318, American Concrete Institute, , Farmington Hills, MI, USA, 2014.
[24] MOHURD (Ministry of Housing and Urban-Rural Development of the People's Republic of China), "Technical standard for precast reinforced concrete shear wall structure assembled by anchoring closed loop reinforcement," China Architecture & Building Press, Beijing, China, JGJ/T 430-2018 in Chinese, 2018.
[25] Y. T. Yu, Y. Zhao, and Z. Q. Gao, "Experimental research on flexural behavior of reinforced concrete composite slab connected without gap," *Journal of Building Structures*, vol. 40, no. 4, pp. 29–37, 2019, in Chinese.
[26] P. Feng, H. L. Qiang, and L. P. Ye, "Discussion and definition on yield points of materials, members and structures," *Engineering Mechanics*, vol. 34, no. 3, pp. 36–46, 2017, in Chinese.
[27] W. Huang, X. Ma, B. Luo, Z. Li, and Y. Sun, "Experimental study on flexural behaviour of lightweight multi-ribbed composite slabs," *Advances in Civil Engineering*, vol. 2019, Article ID 1093074, 11 pages, 2019.
[28] H. Hou, K. Ji, W. Wang, B. Qu, M. Fang, and C. Qiu, "Flexural behavior of precast insulated sandwich wall panels: full-scale tests and design implications," *Engineering Structures*, vol. 180, pp. 750–761, 2019.
[29] J. D. R. Joseph, J. Prabakar, and P. Alagusundaramoorthy, "Precast concrete sandwich one-way slabs under flexural loading," *Engineering Structures*, vol. 138, pp. 447–457, 2017.